Head-to-head comparison of [68Ga]Ga-DOTA.SA.FAPi with [18F]F-FDG PET/CT in radioiodine-resistant follicular-cell derived thyroid cancers

Sanjana Ballal
All India Institute of Medical Sciences
Madhav Yadav
All India Institute of Medical Sciences
Nicky Wakade
All India Institute of Medical Sciences
Frank Roesch
Mainz University: Johannes Gutenberg Universitat Mainz
Euy Sung Moon
Mainz University: Johannes Gutenberg Universitat Mainz
Marcel Martin
Mainz University: Johannes Gutenberg Universitat Mainz
Parvind Sheokand
All India Institute of Medical Sciences
Shipra Agarwal
All India Institute of Medical Sciences
Madhavi Tripathi
All India Institute of Medical Sciences
Ranjit Kumar Sahoo
All India Institute of Medical Sciences
Chandrasekhar Bal (csbal@hotmail.com)
All India Institute of Medical Sciences https://orcid.org/0000-0003-4378-5584

Research Article

Keywords: [68Ga]Ga-DOTA.SA.FAPi; [18F]F-FDG; radioiodine-resistant follicular-cell derived thyroid cancer

Posted Date: February 6th, 2023

DOI: https://doi.org/10.21203/rs.3.rs-2382675/v1

Abstract

Purpose

[^{18}F]F-FDG is a standard and valuable diagnostic imaging modality for radioiodine-resistant follicular-cell derived thyroid cancers (RAI-R FCTC). Recently, molecular imaging probes targeting cancer-associated fibroblasts (CAFs) have gained prominence and have proved to be a potential alternative to [^{18}F]F-FDG PET/CT in oncological imaging. This study aimed to compare the diagnostic efficacy of [^{68}Ga]Ga-DOTA.SA.FAPi and [^{18}F]-FDG PET/CT in RAI-R FCTC patients.

Methods

The retrospective study included 117 RAI-R FCTC patients [68 females, 49 males; mean age: 53.2 ± 11.7 years]. Qualitative assessment parameters included comparing patient-based and lesion-based visual interpretation of both scans. The quantitative assessment included comparing standardized uptake values corrected for lean body mass (SULpeak and SULavg). The findings on both scans were validated with the morphological findings of the diagnostic computed tomography.

Results

60 had single remnants, and 9 had bilateral remnant lesions with a complete concordance in the detection rate on both PET scans. [^{68}Ga]Ga-DOTA.SA.FAPi showed a higher detection efficiency rate for lymph nodes (sensitivity 95.4% vs 86.6%, $p < 0.0001$), liver metastases (100% vs. 81.3%; $p < 0.0001$), brain metastasis (100% vs. 43.4%; p-0.0003). Except for brain metastasis (SULpeak [^{68}Ga]Ga-DOTA.SA.FAPi vs. [^{18}F]-FDG: 13.9 vs. 6.7) and muscle metastasis (SULpeak FAPI vs. FDG: 9.56 vs. 5.62), there was no significant difference in the median SUL uptake values between the radiotracers.

Conclusion

[^{68}Ga]Ga-DOTA.SA.FAPi showed a superior detection efficiency for lymph nodes, liver, bowel, and brain metastasis. Unlike [^{18}F]F-FDG, [^{68}Ga]Ga-DOTA.SA.FAPi can be used as theranostic probes in RAI-R FCTC. [^{68}Ga]Ga-DOTA.SA.FAPi provided a complimentary benefit to the [^{18}F]F-FDG-PET/CT scan in the imaging of RAI-R FCTC.

Introduction

Thyroid cancer is the most common endocrine malignancy with a 3:1 female-to-male ratio (1). Thyroid cancers derived from the follicular cells are classified into papillary thyroid cancer (most common, 80–85%), follicular thyroid cancer (10–15%), poorly differentiated thyroid cancer (< 2%) and undifferentiated (anaplastic) thyroid cancer (< 2%) (2). Surgical management followed by radioiodine (RAI) therapy has remained the mainstay treatment option in treating differentiated thyroid cancer (DTC) patients. DTC metabolizes radioiodine based on the principle of sodium iodide symporter mechanism (NIS) and can be treated with radioiodine. On the other hand, dedifferentiated and other thyroid cancers do not express NIS and hence cannot metabolize radioiodine which is also termed RAI negative or radioiodine refractory thyroid cancer. Approximately 5 to 15% of locoregional DTC and 40–50% of metastatic DTCs are refractory to RAI (1, 3, 4). Several pathways contribute to non-radioiodine concentration in thyroid cancer (TC). One such scenario is the advanced stage thyroid cancer, which has a higher rate of tumor differentiation and loses the NIS expression due to silencing of genes in the NIS pathway, but metabolizes glucose with glucose transporter receptor Type 1 (GLUT − 1) expression. Hence, [^{18}F]F-FDG is taken up in malignant cells with high glucose metabolism (5). The flip-flop phenomenon of high glucose uptake and low iodine uptake is observed in dedifferentiated thyroid cancer and other aggressive variants of thyroid cancer, with poorly differentiated, Hürthle cell cancer, and aggressive variants of thyroid cancer (6–8). To date, [^{18}F]F-FDG has been the standard and valuable diagnostic imaging modality for radioiodine-negative thyroid cancer. [^{18}F]F-FDG PET/CT has a sensitivity and specificity of 84% and 78% in the detection of RAI refractory disease (9). Although [^{18}F]F-FDG PET/CT is a strong indicator of the aggressiveness of thyroid cancer, false-positive findings are a caveat that is observed in approximately 39% of patients (10).

Apart from genetic alterations, recent data suggested that the development, growth, and progression of thyroid cancer are majorly contributed and depend on the cellular pathways involving the interaction of tumor cells and their surrounding tumor microenvironment (TME) (11). Cancer-associated fibroblasts (CAFs) are the key elements of TME and play a critical role in the progression of human cancers. As compared to normal thyroid tissue, CAFs are abnormally increased in thyroid carcinomas.

Studies examining the expression of CAFs in human thyroid cancer tissue have demonstrated a strong correlation between the expression of CAF-affiliated proteins and clinic-pathological features. Cho et al. (12) reported that the presence of CAFs was a significant predictive marker for lymph node metastases in thyroid cancer. Another study by Sun et al. (13) demonstrated that the presence of BRAFV600E mutation in thyroid cancer exhibited high expression of some CAF-related proteins, such as Fibroblast Activation Protein-α (FAP-α). Sun et al. (13) additionally reported that stromal positivity for PDGFR-β was associated with shorter overall survival in PTC.

Targeting CAFs to image or treat cancers is directed either by interfering with the activation of CAFs or inhibiting CAF functions. The FAP inhibitors (FAPI), developed as small molecule radioligands, both for positron emission tomographic (PET) imaging and as a radioligand therapy option, are being explored in many cancers. Recently, molecular imaging probes targeting cancer-associated fibroblasts (CAFs) have gained prominence and have proved to be a potential alternative to [^{18}F]F-FDG PET/CT in oncology imaging. In particular, the FAP inhibitor structures based on the UAMC 1110 motif by Veken et al. (14) combine high selectivity to FAP and low affinity to related members of the protease family. Over the past few years, a series of radiopharmaceuticals based on this FAP inhibitor was developed from various research centers including the [^{68}Ga]Ga-labelled FAPI-02 (15),-04 (16), -46 (17), DOTA.SA.FAPi (18) and DOTAGA.(SA.FAPi)$_2$ (19) and have gained momentum for imaging various cancers. Studies have reported variable uptake patterns of various FAPi radiopharmaceuticals in thyroid cancers with high uptake profiles by a few authors (18) and minimal uptake by Giesel et al. (15) and Kratochwil et al (16).

Scarce-approved options for the treatment of dedifferentiated aggressive thyroid cancers warrant the development of theranostic probes that offers a multifaceted provision for both imaging and treatment of thyroid cancer (20). With only a handful of [^{68}Ga]Ga-FAPI reports on thyroid cancer outlined in the literature, in this study we aim to throw light exclusively on the role of [^{68}Ga]Ga-DOTA.SA.FAPi imaging in the worst outcome patients of thyroid cancer who are radioiodine resistant and compare the diagnostic efficacy of [^{68}Ga]Ga-DOTA.SA.FAPi and [^{18}F]F-FDG PET/CT in radioiodine-resistant follicular-cell derived thyroid cancer patients.

Materials And Methods

This reterospective study was approved by the institute ethics committee of All India Institute of Medical Sciences, New Delhi, India. Patients were enrolled between April 2019 to October 2022. It is a collaboration between the Department of Nuclear Medicine, Medical Oncology Department at All India Institute of Medical Sciences, and the Department of Chemistry, Johannes Gutenberg University, Mainz, Germany, which provided the labeling precursor as depicted in Fig. 1.

Synthesis Of [ga]ga-dota.sa.fapi And Quality Control

Radiolabeling of [^{68}Ga]Ga-DOTA.SA.FAPi was conducted as detailed in our previous publications (18) and detailed in supplementary data.

Definition Of Radioiodine-resistant Thyroid Cancer (Rai-r Fctc)

Radioiodine resistant follicular-cell thyroid cancer (RAI-R FCTC) refers to the following scenarios: all follicular cell-derived thyroid cancer with loss of thyroid differentiation features including negative RAI whole body scan, radioiodine refractory DTC metastases progressing despite radioiodine uptake, persistent disease in DTC patients despite cumulative I-131 of > 22.2GBq (600 mCi), one or more lesions did not demonstrate radioactive iodine uptake, the disease never concentrates radioiodine, de-novo radioiodine refractory disease, and a combination of FDG positive, elevated thyroglobulin, and I-131 negative lesions (TENIS syndrome).

Patients fulfilling the following eligibility criteria were enrolled in the study: patients with histologically proven follicular-cell derived thyroid cancer, patients with RAI-R FCTC, and patients who underwent both [^{18}F]F-FDG, [^{68}Ga]Ga-DOTA.SA.FAPi PET/CT within a time interval of one month, and patients who provided the written informed consent form. Pregnant and lactating women were excluded from the study. According to the eligibility criteria, 91 patients were included in the study. Patients fasted at least 6 hours before the [^{18}F]F-FDG injection, but no preparation was required for [^{68}Ga]Ga-DOTA.SA.FAPi PET/CT scan. A normal blood glucose level in the peripheral blood was ensured before [^{18}F]F-FDG PET/CT evaluation. Mean activities of 270 MBq (range: 185 to 370 MBq) [^{18}F]F-FDG and 180 MBq (range: 59.2 to 321 MBq) [^{68}Ga]Ga-DOTA.SA.FAPi radiotracers were injected. Scans were acquired on a 128-slice GE Discovery 710* 128 Slice PET/CT scanner. The details of acquisition and processing are mentioned in supplementary materials. A diagnostic CT scan was used as the reference standard, and the uptake in the lesions on both scans was compared with the morphological features.

Definitions

• True-positive (TP) lesion: active uptake in the lesion seen on [^{18}F]F-FDG / [^{68}Ga]Ga-DOTA.SA.FAPi PET/CT images and found to be positive on diagnostic CT/histological examination.

• False-positive (FP) lesion: active uptake in the lesion seen on [^{18}F]F-FDG / [^{68}Ga]Ga-DOTA.SA.FAPi PET/CT images and found to be negative on diagnostic CT/ histological examination/clinical or radiological follow-up.

• True-negative (TN) lesion: No uptake seen on [^{18}F]F-FDG / [^{68}Ga]Ga-DOTA.SA.FAPi PET/CT images and the results on diagnostic CT/histological examination/clinical or radiological follow-up were also negative.

• False-negative (FN) lesion: lesion that was missed in [^{18}F]F-FDG / [^{68}Ga]Ga-DOTA.SA.FAPi PET/CT images but was found to be positive for malignancy at diagnostic CT/histological examination/clinical or radiological follow-up.

Statistical Analysis

Continuous variables were presented in terms of mean, median, standard deviation (SD), range, and interquartile range (IQR). [^{18}F]F-FDG and [^{68}Ga]Ga-DOTA.SA.FAPi uptakes were compared using paired Student's t-test or Wilcoxon signed-rank test. The sensitivity, specificity, and accuracy of [^{18}F]F-FDG and [^{68}Ga]Ga-DOTA.SA.FAPi PET/CT examinations were calculated and compared. Statistical difference in the detection rate of primary tumors, lymph nodes, and visceral metastases between [^{18}F]F-FDG and [^{68}Ga]Ga-DOTA.SA.FAPi scans were analyzed by the McNemar test. Statistical analysis was performed using MedCalc statistical software.

Results

One Hundred and seventeen RAI-R FCTC patients [68 females and 49 males] with a mean age of 53.2 ± 11.7 years (range: 24 to 84 years) were included in the study. Eighty-Five (72.65%) patients had RR-DTC disease, one patient (0.85%) had Hurthle/Oncocytic thyroid cancer and the remaining thirty-one (26.5%) patients had poorly differentiated thyroid cancer. Post intravenous injection of [^{68}Ga]Ga-DOTA.SA.FAPi, all vital parameters remained normal and no adverse events were noted. Detailed histopathology diagnosis is enumerated in Table 1.

Table 1
The detailed histopathology of the types of RAI-R FCTC.

HPE of thyroid cancer	**Number of patients (n = 117)**
RR-DTC	
Classic PTC	53 (45.30%)
FVPTC	8 (6.84%)
FTC	16 (13.68%)
PTC + FTC	5 (4.28%)
Tall cell variant PTC	3 (2.56%)
Hurthle/Oncocytic thyroid Cancer	1 (0.85%)
Poorly differentiated thyroid cancer	
Insular	4 (3.42%)
PDTC	11 (9.37%)
FVPTC + PDTC*	4 (3.42%)
FVPTC + insular*	1 (0.85%)
PTC + PDTC*	6 (5.13%)
PDTC + insular*	2 (1.71%)
FTC + PDTC*	2 (1.71%)
PTC + insular*	1 (0.85%)
FVPTC: Follicular variant of papillary thyroid carcinoma; FTC: follicular thyroid carcinoma, PDTC: poorly differentiated thyroid cancer.	
*Differentiated component is present,	

Primary tumor

Among the 117 patients, 60 had single remnants, and 9 had bilateral remnant lesions with complete concordance in the detection rate between both radiotracers. The median SUL values were also comparable between the tracers {SULpeak [^{68}Ga]Ga-DOTA.SA.FAPi: 10.82; (IQR: 5.11 to 22. 2), vs [^{18}F]F-FDG: 7.86; (IQR: 4.15 to 20.84, p-0.263)} (Table 2).

Table 2
Comparison between [^{68}Ga]Ga-DOTA.SA.FAPi and [^{18}F]F-FDG standardized uptake values in various locations of metastasis.

Location of primary/metastasis	No of patients	No of primary/metastasis	[^{68}Ga]Ga-DOTA.SA.FAPi (SULpeak)	[^{18}F]F-FDG (SULpeak)	P-value	[^{68}Ga]Ga-DOTA.SA.FAPi (SULavg)	[^{18}F]F-FDG (SULavg)	P-value
Thyroid remnant	69 (60%)	78	10.82 [5.11 to 22.2]	7.86 [4.15 to 20.84]	0.263	5.91 [2.80 to 7.99]	3.76 [1.84 to 15.28]	0.167
Lymph nodes	99 (84.61%)	537	6.86 [3.21 to 12.72]	5.018 [2 to 10.17]	0.286	3.42 [2.02 to 6.28]	2.05[1.01 to 6.32]	0.1931
Lung metastasis	82 (70.08%)	-	5.64 [2.23 to 10.95]	4.96 [2.11 to 10.22]	0.4274	3.60 [1.25 to 7.25]	3.63 [1.88 to 5.77]	0.9589
Bone metastasis	53 (45.3%)	< 6 sites n = 14 6–20 n = 31 > 20 n = 8	8.24 [5.62 to 14.82]	6.9 [3.17 to 13.1]	0.1830	4.22 [2.48 to 7.51]	3.47[1.97 to 7.39]	0.2424
Liver metastasis	30 (25.6%)	107	7.28 [4.82 to 12.31]	5.97 [3.01 to 7.95]	0.212	4.01 [2.80 to 7.2]	2.16 [1.38 to 3.37]	0.1016
Brain metastasis	11 (9.4%)	23	13.9 [6.89 to 28.7]	6.7 [2.24 to 9.23]	0.0001	6.89 [2.1 to 9.23]	3.23 [1.1 to 6.72]	0.0001
Pleural metastasis	11 (9.4%)	-	5.82 [3.2 to 8.6]	6.45 [2.13 to 10.1]	0.486	2.63 [1.86 to 4.1]	3.1 [1.33 to 6]	0.534
Muscle metastasis	3 (2.5%)	6	9.56 [8.32 to 12.06]	5.62 [4.9 to 6.89]	0.0085	6.1 [4.86 to 8.61]	3.33 [2.9–4.2]	0.0266
Bowel metastasis	1 (0.8%)	2	-	-	-	-	-	-

Lymph Node Metastases

Ninety-nine patients (84.61%) out of 117 patients had a total of 537 lymph node (LN) metastasis on computed tomography. While [^{68}Ga]Ga-DOTA.SA.FAPi correctly diagnosed 95.4% (512/537) of LN metastases [TP: 467, TN: 16 patients, FP: 4; FN: 25], [^{18}F]F-FDG diagnosed 86.6% (465/537) [TP:432, TN:16 patients, FP:17, FN: 72]; $p < 0.0001$. The difference between the proportions of detection of lymph nodes was 8.7% (95%CI: 2.77% – 7.15%), chi-square value 24.1%, $p < 0.0001$. However, The SULpeak values of the LN's were not different between the radiotracers {SUVmax; [^{68}Ga]Ga-DOTA.SA.FAPi: 6.86 (3.21 to 12.72) vs. [^{18}F]F-FDG: 5.018 (2 to 10.17; p-0.286}(Table 2).

Lung Metastases

Eighty-two (70.08%) patients were detected with lung metastasis on CT, [^{68}Ga]Ga-DOTA.SA.FAPi showed concordant findings in sixty seven (81.7%) patients while [^{18}F]F-FDG has shown complete concordant findings in Fifty-three (69.6%) patients. On detailed analysis, [^{68}Ga]Ga-DOTA.SA.FAPi failed to show expression in eleven (12.8%) and mixed uptake [TP + FN] in four patients. Complete discordant uptake was observed on [^{18}F]F-FDG scans with no FDG uptake in eleven patients with CT-positive lung metastases and a mixed uptake pattern in 18 patients [TP + FN: n = 12, TP + TN + FP: n = 2, TP + FP: n = 4]. A complete discordance in the uptake of radiotracers was noted where [^{68}Ga]Ga-DOTA.SA.FAPi in line with the CT scan findings did not demonstrate any uptake, but false-positive uptake on [^{18}F]F-FDG in the lung was noted in seven patients, corresponding to infective sequelae (Fig. 2). Interestingly in five patients with radiological lung metastases, both FAPI and FDG scans showed no activity of radiotracers. Four among them had RR-DTC and one patient had poorly differentiated histology.

Bone Metastases

Bone lesions were classified according to the number of bone metastasis (Table 1). Among the 53 (45.3%) patients with bone metastases, the number of bone metastases was less than 6 in fourteen patients, between 6 to 20 in 31 patients, and > 20 in eight patients. Both radiotracers documented complete concordance in detection and a similar uptake value between the radiotracers {SULpeak: 8.24 [5.62 to 14.82] vs. 6.9 [3.17 to 13.1], p-0.1830} (Table 2).

Liver Metastases

107 liver metastases were detected in thirty patients and [^{68}Ga]Ga-DOTA.SA.FAPi correctly diagnosed all the metastasis. On the other hand, [^{18}F]F-FDG could detect only 87 (81.3%) liver lesions, among whom [^{18}F]F-FDG completely failed to detect any liver metastases in three patients. (Fig. 3&4) Significant discordant findings were noted in the poorly differentiated category where [^{68}Ga]Ga-DOTA.SA.FAPi detected all forty-six liver metastases, [^{18}F]F-FDG could detect only twenty-one ($p < 0.0001$)

Other Distant Metastases

Pleural metastases were detected in eleven patients with similar detection rates and uptake patterns in both radiotracers. One patient had bowel metastasis that was missed on [^{18}F]F-FDG due to physiological interference but was delineated on [^{68}Ga]Ga-DOTA.SA.FAPi scan. Muscle metastases were detected in three patients with 6 sites on both scans, but the uptake was on [^{68}Ga]Ga-DOTA.SA.FAPi scan was higher than that of [^{18}F]F-FDG. Eleven patients had 23 brain metastases, which were completely missed on [^{18}F]F-FDG in two patients. Concerning brain metastases the sensitivity of [^{68}Ga]Ga-DOTA.SA.FAPi was 100% compared with 43.4% (9/23) for [^{18}F]F-FDG PET/CT (p-0.0003). Interestingly, the [^{68}Ga]Ga-DOTA.SA.FAPi derived SUL values were two-fold higher than [^{18}F]F-FDG in the brain metastasis {SULpeak: 13.9 (6.89 to 28.7) vs. 6.7 (2.24 to 9.23); p-0.0001} (Table 2).

Discussion

Aggressive thyroid cancer patients exhaust radioiodine therapy as a theranostic option. About 8 decades after the introduction of radioiodine, radiopharmaceuticals based on fibroblast activation protein inhibitors have shown a role in theranostics of thyroid cancer.

The present study compared to diagnostic efficacy of [^{68}Ga]Ga-DOTA.SA.FAPi with [^{18}F]F-FDG-PET/CT in patients with RAI-R FCTCs. It aimed to conduct a systematic evaluation of the difference between FAPi expression and Glucose uptake in the detection of RAI-R FCTC. [^{68}Ga]Ga-DOTA.SA.FAPi showed a higher detection efficiency rate for lymph nodes (sensitivity 95.7% vs 88.6%, $p < 0.0001$), liver metastases (100% vs. 72%; $p < 0.0001$), and brain metastases (100% vs. 38.8%; p-0.0003). Overall the results suggest that [^{68}Ga]Ga-DOTA.SA.FAPi has higher detection rates in terms of the number of lymph nodes, liver, lung, and brain metastases as compared to [^{18}F]F-FDG PET/CT.

Although the semi-quantitative parameters such as SULpeak and average values for various metastatic sites were similar between the two radiotracers, [^{68}Ga]Ga-DOTA.SA.FAPi showed the values were substantially superior values for brain and muscle metastases. Similarly, irrespective of the type of FAPi molecule several studies have indicated the favorable property of [^{68}Ga]Ga-FAPi PET scans of low uptake in the normal parenchyma which is beneficial for tumor delineation in particular in the head and neck and liver regions in different cancers (21–23).

Loco-regional lymph node (LN) metastasis is typically one of the initial sites of disease progression in thyroid cancer which eventually progresses to the distant organs. Among the various diagnostic modalities, ultrasonography limits the diagnosis of central compartment lymph nodal metastases as certain LNs are deeply seated around the trachea and overlapped by surrounding structures resulting in false

negative results. Currently, though [^{18}F]F-FDG PET/CT is the modality of choice in evaluating RR-DTC and other non-iodine concentrating aggressive variants of thyroid cancer such as Hürthle, insular, PDTC, and ATC, but its use is limited in inflammatory lymphadenopathy which has higher false positive rates. Our study demonstrated that [^{68}Ga]Ga-DOTA.SA.FAPi PET/CT was capable of detecting lymph node metastases more reliably than was [^{18}F]FDG PET/CT (Table 2). This achievement is in agreement with data published previously by Wang et al (23). According to their reports, [^{68}Ga]Ga-FAPi PET/CT imaging can detect lymph node metastases at an earlier stage and has the potential to increase occult lymph node metastasis detection, guiding the more accurate staging of thyroid cancer patients consistent with the higher specificity of the former technique.

[^{18}F]F-FDG exhibited relatively low sensitivity for small metastatic lesions and low specificity for infective lung pathology. Similarly, [^{68}Ga]Ga-DOTA.SA.FAPi also demonstrated mixed uptake in lung metastases. False-negative results in lung metastases were observed on both radiotracers, but in higher percentages on [^{18}F]F-FDG compared to [^{68}Ga]Ga-FAPi. One possible explanation could be the rapid [^{18}F]F-FDG efflux from the tumor cells in highly aggressive metastases. Alternatively, minimal to no uptake in the lung metastases on both radiotracers could be due to the size of the lesions and breathing artifacts. From this standpoint, it remains clear that breathold CT scan with careful clinical follow-up is still an invaluable approach to diagnose small lung nodules with indeterminate uptake on both radiotracers. Further, studies should be conducted in detail regarding this uptake pattern in various subtypes of thyroid cancers.

Diagnosis and detection of PDTC have been controversial from the histopathological staging to the imaging point of view (24). These ambiguities have also made management difficult. Unlike [^{18}F]F-FDG in RR-DTC, its role is not clearly outlined as imaging of choice by the American Thyroid Association (ATA). However, the role of FDG in PDTC is not well researched. Though more often PDTC is an FDG-positive tumor, some studies have shown an intermediate GLUT1 expression and FDG uptake with values between DTC and ATC (25). The remarkably high detection rate of FAPi in PDTC and ATC in all the metastatic sites compared to FDG has unveiled a new option for imaging these aggressive variants which has controversial results involving different uptake patterns and intermediate FDG expression. With FAPI positive expression in all the PDTC lesions, it opens new avenues for systemic treatment options in a patient with limited treatment options or scarce treatment options.

An interesting case to discuss is a case of a 66-year-old female (Fig. 3) with known poorly differentiated thyroid carcinoma who underwent [^{18}F]F-FDG PET/CT for follow-up. A, images from the [^{18}F]F-FDG PET/CT scan demonstrate minimal [^{18}F]F-FDG uptake in the bilateral lung metastases and normal findings in the rest of the organs (Fig. 3A). CT scan axial sections reveal bilateral lung nodules and liver metastases (Fig. 3B). [^{68}Ga]Ga-DOTA.SA.FAPi PET/CT was performed for further evaluation and scan findings reveal intense uptake in bilateral lung nodules, and multiple liver lesions (Fig. 3C). [^{68}Ga]Ga-DOTA.SA.FAPi upscaled the detection of metastases in the lung and liver. Highly aggressive tumors compose 90% of tumor stroma rather than the tumor itself. Hence low glycolytic activity and higher expression of FAPi may be the reason for these discordant findings.

Another case (Fig. 4) of the complementary benefit of imaging with both [^{18}F]F-FDG PET/CT and [^{68}Ga]Ga-FAPi PET/CT is described as follows: In a 65-year-old female with RR-DTC, mediastinal LNs showed intense [^{18}F]F-FDG uptake which was negligible on [^{68}Ga]Ga-DOTA.SA.FAPi PET/CT, on the contrary intense [^{68}Ga]Ga-DOTA.SA.FAPi accumulation was noted in the bilateral lung nodules, liver, and pelvic bone metastases. The diagnostic accuracy improved significantly with a complimentary dual scan approach in this patient with a combination of true positive, false positive, true negative, and false negative on both scans.

Few studies have explored the role of different [^{68}Ga]Ga-labelled FAPi molecules in thyroid cancers which are limited to only a few cases per study. Contrary to our findings, few researchers did not observe the utility of [^{68}Ga]Ga-DOTA.SA.FAPi in low RAI expressing thyroid cancer and demonstrated low parenchymal uptake in RR-DTC. Kratochwil et al. (16) observed low uptake of ^{68}Ga-FAPI-04 in a few cancers including differentiated thyroid cancer with uptake rates (SUVmax < 6). Similarly, Giesel et al. (15) observed dedifferentiated thyroid cancer with flip-flop uptake of [^{18}F]F-FDG was not accumulating [^{68}Ga]Ga-FAPi-04. Huang et al. (26) also observed that patients with iodine uptake negative thyroid cancer exhibited low [^{68}Ga]Ga-FAPi tracer uptake compared with [^{18}F]F-FDG PET. At the current stage, [^{18}F]F-FDG PET/CT is still the PET radiopharmaceutical of choice with its wide availability, cost-effectiveness, and standardization of quantification techniques for restaging, and [^{68}Ga]Ga-FAPi now only has a complementary role.

Although imaging of [^{68}Ga]Ga-FAPi molecules has proved promising imaging radiotracers, the same monomeric compounds when labeled to therapeutic counter parts have shown rapid washout of the radiotracers from the tumor. To improve the tracer kinetics for introducing FAPi-based therapeutic avenues, Moon et al. structurally modified and optimized the monomeric FAPi precursor to homodimeric compounds and successfully showed prolonged tumor retention time (19). Eventually, the same group studied the dosimetry and pharmacokinetics of [^{177}Lu]Lu-DOTAGA.(SA.FAPi)$_2$ homodimeric compound in RR-DTC patients which significantly prolonged tumor retention even up to 168 h, post-treatment (20). However, the study included only RR-DTC patients and future research should focus and explore on the expansion of this

treatment option in various radioiodine-resistant thyroid cancer (RAI-R TC) with broader histological variants. Long-term outcomes of [^{177}Lu]Lu-FAPi treatment in various TC's will accurately reflect and will be the answer to the utility of the treatment.

Limitations

Our study had some limitations. Firstly, the study majorly included classic RR-DTC (60%) and small sample sizes concerning histological subtypes of other non-iodine concentrating thyroid cancers which results in low evidence results. For data to clinically translate well it would require well-executed clinical trials with larger sample sizes of each histological subtype of TC and stringent eligibility criteria. Second, contrast-enhanced computed tomography CECT scans were not acquired in all patients. Thirdly, gold standard HPE validation was not performed in discrepant lesions, and fourthly, was beyond the scope of work as a biopsy from each lesion was impractical.

Conclusion

In this study, we compared the PET tracer [^{68}Ga]Ga-DOTA.SA.FAPi having high-affinity and highly selective FAP inhibitor with [^{18}F]F-FDG in various RAI-R FCTCs. The very low physiological uptake of [^{68}Ga]Ga-DOTA.SA.FAPi particularly increases the chance of detecting hepatic and brain metastases. Overall, [^{68}Ga]Ga-DOTA.SA.FAPi PET/CT demonstrated lower false positive and false negative rates as compared to [^{18}F]F-FDG. Similar to [^{18}F]F-FDG, [^{68}Ga]Ga-DOTA.SA.FAPi is a useful diagnostic modality for both diagnosis and from a theranostic point of view. The prevalence of false positive and false negative in both scans unfolds the necessity of a complementary dual scan approach to staging any thyroid cancer. The highly selective uptake of [^{68}Ga]Ga-DOTA.SA.FAPi in the tumors has a promising future for the precision treatment of various FAPI-positive cancers. This finding may be significant as it paves the way for future studies investigating the role of [^{68}Ga]Ga-DOTA.SA.FAPi PET/CT guided ^{177}Lu/^{90}Y/^{225}Ac-FAPi treatment in aggressive dedifferentiated variants in whom no options of TKIs are available. Unlike FDG which can be used for only imaging, the effective targeting of thyroid CAFs with radiolabeled [^{68}Ga]Ga-DOTA.SA.FAPi appears to be an emerging theranostic option and a significant step moving towards precision treatment in various radioiodine-resistant thyroid cancers.

Declarations

Competing Interests: The authors have no relevant financial or non-financial interests to disclose

Author Contributions: *All authors contributed to the study conception and design. Material preparation, data collection and analysis were performed by Sanjana Ballal, Madhav Prasad Yadav, Nicky Wakade, and Parvind Sheokand. The first draft of the manuscript was written by Sanjana Ballal, and Madhav Prasad Yadav. Images were processed and reported by Chandrasekhar Bal and Madhavi Tripathi.* Shipra Agarwal reviewed the pathology reports. Dr. Ranjit Kumar Sahoo referred patients for scans. Frank Roesch, Euy Sung Moon, Marcel Martin are our collaborators from the university of Mainz and have synthesized the precursor, and finalized the manuscript. *All authors commented on previous versions of the manuscript. All authors read and approved the final manuscript.*

Data Availability: The datasets generated during and/or analyzed during the current study are available from the corresponding author on reasonable request.

Disclosures: The authors have nothing to disclose.

Conflict of Interest: the authors have no conflict of interest

Ethical Clearance: Ethical clearance received Ref No: **IECPG:22/27**

Informed Consent: A written informed consent was obtained from all patients to participate in the study, use clinical information to analyze data, and use images for the purpose of publication.

Support: None

Disclaimer: This work has not been submitted elsewhere as a full article and is not under consideration by any other journal.

References

1. Zarnegar R, Brunaud L, Kanauchi H, et al. Increasing the effectiveness of radioactive iodine therapy in the treatment of thyroid cancer using trichostatin A, a histone deacetylase inhibitor. Surgery. 2002;132:984–90.

2. Dralle H, Machens A, Basa J, Fatourechi V, Franceschi S, Hay ID, et al. Follicular cell-derivbed thyroid cancer. Nat Rev Dis Primers. 2015; 10;1:15077.
3. Worden F. Treatment strategies for radioactive iodine refractory differentiated thyroid cancer. Ther Adv Med Oncol. 2014;6:267–79.
4. Xing M, Haugen BR, Schlumberger M. Progress in molecular-based management of differentiated thyroid cancer. Lancet. 2013;381:1058–69.
5. Choudhury PS, Gupta M. Differentiated thyroid cancer theranostics: radioiodine and beyond. Br J Radiol. 2018; 91: 20180136.
6. Deandreis D, Al Ghuzlan A, Leboulleux S, et al. Do histological, immunohistochemical, and metabolic (radioiodine and fluorodeoxyglucose uptakes) patterns of metastatic thyroid cancer correlate with patient outcome? Endocr. Relat. Cancer. 2011; 18:159–69.
7. Rosenbaum-Krumme SJ, Görges R, Bockisch A, et al. ^{18}F-FDG PET/CT changes therapy management in high-risk DTC after first radioiodine therapy. Eur J Nucl Med Mol. Imaging. 2012;39:1373–80.
8. Grewal RK, Ho A, Schöder H. Novel approaches to thyroid cancer treatment and response assessment. Semin. Nucl. Med. 2016;46:109–118.
9. Klain M, Zampella E, Nappi C, et al. Advances in Functional Imaging of Differentiated Thyroid Cancer. Cancers. 2021; 13:4748.
10. Boellaard R, Delgado-Bolton R, Oyen WJ, et al. European Association of Nuclear Medicine (EANM) FDG PET/CT: EANM procedure guidelines for tumour imaging: Version 2.0. Eur. J. Nucl. Med. Mol. Imaging. 2015; 42:328–54.
11. Fozzatti L, Cheng SY. Tumor cells and cancer associated fibroblasts: a synergistic crosstalk to promote thyroid cancer. Endocrinol Metab (Seoul).*2020;*35:673–80.
12. Cho JG, Byeon HK, Oh KH, et al. Clinicopathological significance of cancer-associatedfibroblasts in papillary thyroid carcinoma: a predictive marker of cervical lymph node metastasis. Eur Arch Otorhinolaryngol. 2018;275:2355-61.
13. Sun WY, Jung WH, Koo JS. Expression of cancer-associated fibroblast-related proteins in thyroid papillary carcinoma. Tumour Biol. 2016;37:8197-8207.
14. Jansen K, Heirbaut L, Verkerk R, et al. Extended structure-activity relationship and pharmacokinetic investigation of (4-quinolinoyl)glycyl-2-cyanopyrrolidine inhibitors of fibroblast activation protein (FAP). J Med Chem. 2014;57:3053–74.
15. Giesel FL, Kratochwil C, Lindner T, et al. ^{68}Ga-FAPI PET/CT: Biodistribution and Preliminary Dosimetry Estimate of 2 DOTA-Containing FAP-Targeting Agents in Patients with Various Cancers. J Nucl Med. 2019;60:386-92.
16. Kratochwil C, Flechsig P, Lindner T, et al. ^{68}Ga-FAPI PET/CT: Tracer Uptake in 28 Different Kinds of *Cancer.* J Nucl Med. 2019;60:801-5.
17. Meyer C, Dahlbom M, Lindner T, et al. Radiation dosimetry and biodistribution of 68Ga-FAPI-46 PET imaging in cancer patients. J Nucl Med. 2020; 61:1171–77.
18. Ballal S, Yadav MP, Moon ES, et al. Biodistribution, pharmacokinetics, dosimetry of [68Ga]GaDOTA.SA.FAPi, and the head-to-head comparison with[18F]F-FDG PET/CT in patients with various cancers. Eur J Nucl Med Mol Imaging. 2021;48:1915–31.
19. Moon ES ,Ballal S, Yadav MP, et al. Fibroblast Activation Protein (FAP) targeting homodimeric FAP inhibitor radiotheranostics: a step to improve tumor uptake and retention time. Am J Nucl Med Mol Imaging. 2021;11:476-91.
20. Ballal S, Yadav MP, Moon ES, et al. Novel Fibroblast Activation Protein Inhibitor-Based Targeted Theranostics for Radioiodine-Refractory Differentiated Thyroid Cancer Patients: A Pilot Study. Thyroid. 2022;32:65-77.
21. Pang Y, Zhao L, Luo Z, et al. Comparison of 68Ga-FAPI and 18F-FDG Uptake in Gastric, Duodenal, and Colorectal Cancers. Radiology. 2021;298:393-402.
22. Chen H, Pang Y, Wu J, et al. Comparison of [68Ga]Ga-DOTA-FAPI-04 and [18F] FDG PET/CT for the diagnosis of primary and metastatic lesions in patients with various types of cancer. Eur J Nucl Med Mol Imaging. 2020;47:1820-32.
23. Wang L, Tang G, Hu K, et al. Comparison of 68Ga-FAPI and 18F-FDG PET/CT in the Evaluation of Advanced Lung Cancer. Radiology. 2022;303:191-99.
24. Michael Rivera, Ronald A. Ghossein, et al. Histopathologic characterization of radioactive iodine-refractory fluorodeoxyglucose-positron emission tomography-positive thyroid carcinoma. Cancer. 2008, 113:48-56.
25. Treglia G, Muoio B, Roustaei H, Kiamanesh Z, Aryana K, Sadeghi R. Head-to-Head Comparison of Fibroblast Activation Protein Inhibitors (FAPI) Radiotracers versus [^{18}F]F-FDG in Oncology: A Systematic Review. Int J Mol Sci. 2021;22:11192.
26. Huang R, Pu Y, Huang S, et al. FAPI-PET/CT in Cancer Imaging: A Potential Novel Molecule of the Century. Front Oncol. 2022;12:854658.

Figures

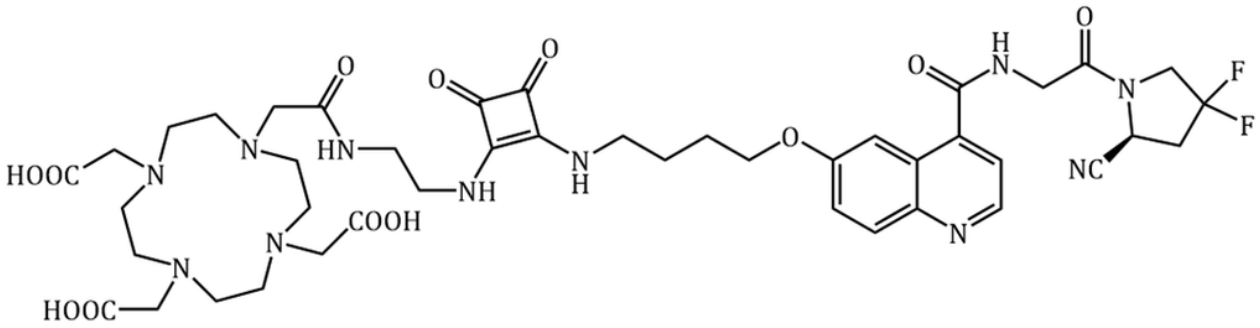

Figure 1

Chemical structure of the labeling precursor DOTA.SA.FAPi

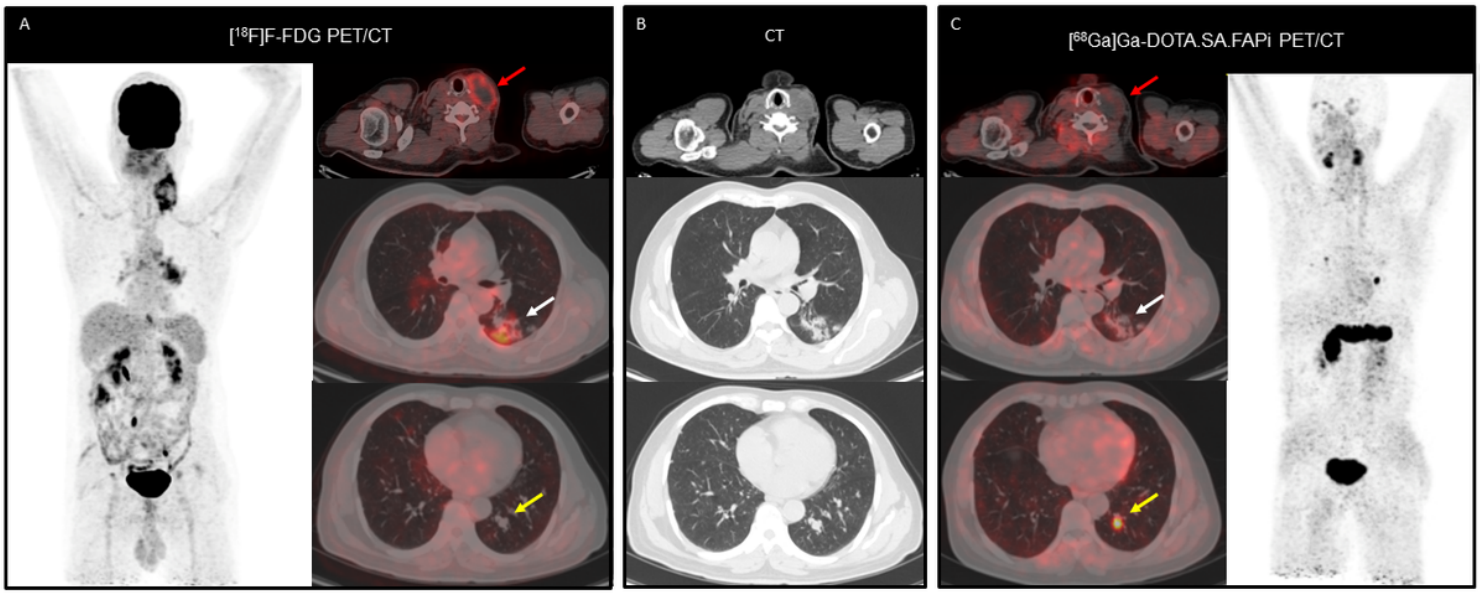

Figure 2

In a A seventy-five year old male patient with anaplactic thyroid carcinoma, peripheral FDG avidity is noted in a large left level III/IV cervical lymph nodal mass measuring 5.4 x 5.2 cm (A, red arrow). Multiple sub-centimetric sized bilateral lung nodules noted with no FDG avidity (A, yellow arrow). Fibrotic changes with intense FDG avidity in the left lung (A (white arrow), B (middle row) is an infective sequele. On the other hand, [^{68}Ga]Ga-DOTA.SA.FAPi did not demonstarte any uptake in the lymph node (C, red arrow), but demonstated intense FAPi expression in the lung metastases (C, yellow arrow) and no uptake in the correponding left lung fibrotic mass (C, white arrow).

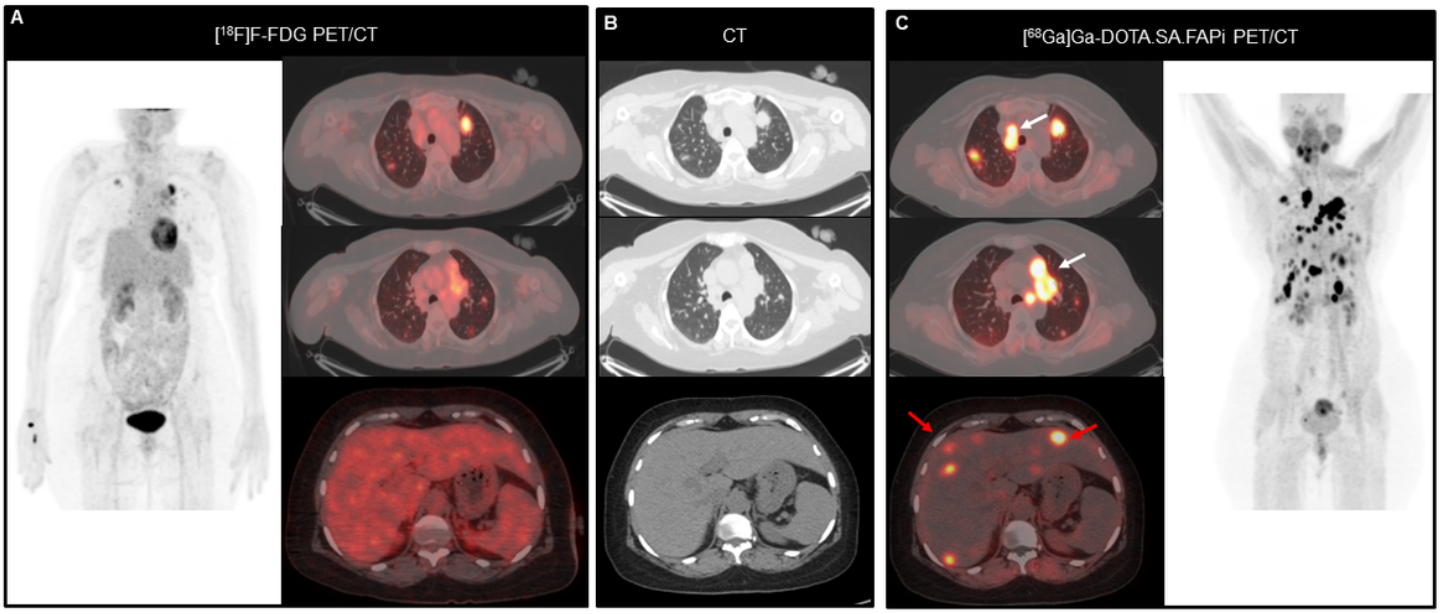

Figure 3

A 66-year-old female was diagnosed with poorly differentiated thyroid carcinoma and underwent [^{18}F]F-FDG PET/CT for follow-up. A, Images from the [^{18}F]F-FDG PET/CT scan demonstrate minimal [^{18}F]F-FDG uptake in the bilateral lung metastases and normal findings in the rest of the organs. B, CT scan axial sections reveal bilateral lung nodules and liver metastases (segment). C, [^{68}Ga]Ga-DOTA.SA.FAPi PET/CT was performed for further evaluation and scan findings revealed intense uptake in bilateral lung nodules and multiple liver lesions.

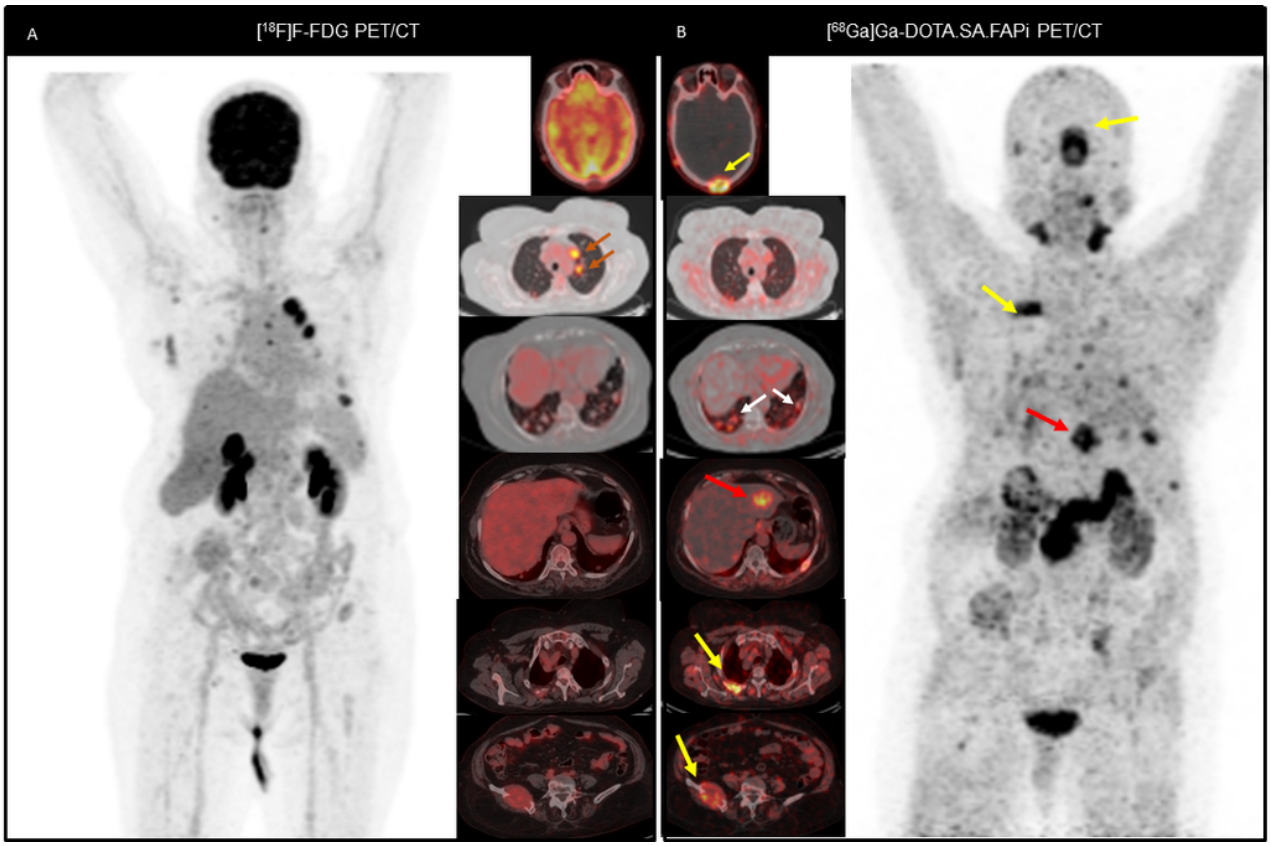

Figure 4

In a 65-year-old female with RR-DTC, A, [^{18}F]F-FDG PET MIP image demonstrated intense FDG uptake in the mediastinal LNs (MIP & CT axial[orange arrows]) which was negligible on [^{68}Ga]Ga-DOTA.SA.FAPi PET/CT. On the contrary [^{68}Ga]Ga-DOTA.SA.FAPi PET/CT (B, C) demonstrated additional FAPi expression in the bilateral lung nodules (white arrows B), liver (red arrows B, C), and bone metastases (yellow arrows B, C) that did not show FDG uptake.

Supplementary Files

This is a list of supplementary files associated with this preprint. Click to download.

- supplementaryinformationEJNMMI15122022.docx